INSTITUTE OF PLASMA PHYSICS

NAGOYA UNIVERSITY

DAISEN SUMMER SCHOOL

(Laser Fusion Workshop)

IPPJ-235 November 1975

RESEARCH REPORT

NAGOYA, JAPAN

DAISEN SUMMER SCHOOL

(Laser Fusion Workshop)

IPPJ-235 November 1975

Further communication about this report is to be sent to the Research Information Center, Institute of Plasma Physics, Nagoya University, Nagoya, JAPAN.

Contents

Preface

During the last month of my visit to Japan as a NSF exchange scientist, I decided to spend a week to serve to organize a workshop to attack problems in the general area of laser-plasma interaction and laser fusion. In response to my proposal, Prof. C. Yamanaka, T. Taniuti and K. Takayama kindly made arrangement for the financial support and the meeting was materialized in July 16 to 22nd, 1975. The arrangement of the meeting including the site selection and other business matters were kindly made by Drs. K. Mima and T. Yamanaka.

The meeting started first by hearing current problems from the experimentalists. Subsequently following five subjects were chosen to attack A) Implosion problem B) Stability of self-focused laser beam, C) Generation mechanism of magnetic field, D) Fusion burner design, and E) Acceleration mechanism of ions.

Each of the invited theorists chose one or more subjects and spent about three and a half days of intensive hours (from 9 am to 11:00 pm) of creative works. Meanwhile experimentalists had series of meeting on future plans.

The site that Dr. Mima chose was most suited for the workshop, beautiful view of Mt. Daisen and Japan sea, complete isolation and good foods. Thanks to the fantastic effort and competence of the participants, extremely fruitful outputs were produced. This report summarizes the results

of the intensive works of the seven days (including the tough climbing of the Mt. Daisen).

Akira Hasegawa
The Principal

List of Participants

Assoc. Prof. Junji Fujita	(Nagoya Univ.)
Prof. Akira Hasegawa	(Nagoya Univ. and Bell Labs.)
Dr. Tadatsugu Hatori	(Nagoya Univ.)
Mr. Takashi Ikuta	(Nagoya Univ.)
Miss. Sanae Inoue	(Tokyo Univ.)
Dr. Masaaki Inutake	(Nagoya Univ.)
Mr. Kimitaka Itoh	(Tokyo Univ.)
Dr. Masashi Kako	(Osaka Univ.)
Dr. Yasuhito Kiwamoto	(Yokohama National Univ.)
Mr. Yuji Kodama	(Nagoya Univ.)
Dr. Kunioki Mima	(Osaka Univ.)
Dr. Jun-ichi Mizui	(Nagoya Univ.)
Assoc. Prof. Sadao Nakai	(Osaka Univ.)
Dr. Katsunobu Nishihara	(Nagoya Univ.)
Prof. Keishiro Niu	(Tokyo Institute of Technology)
Mr. Kazuhiro Nozaki	(Nagoya Univ.)
Mr. Yukiharu Ohsawa	(Nagoya Univ.)
Assoc. Prof. Yukio Sakagami	(Gifu Univ.)
Dr. Eiji Sakai	(Japan Atomic Energy Research)
Dr. Takatomo Sasaki	(Osaka Univ.)
Dr. Kohnosuke Sato	(Nagoya Univ.)
Assoc. Prof. Tetsuya Sato	(Tokyo Univ.)
Prof. Hiroshi Takuma	(Osaka Univ.)
Dr. Toshio Tange	(Hiroshima Univ.)
Prof. Tosiya Taniuti	(Nagoya Univ.)
Dr. Shunsuke Toyama	(Hitachi Ltd. Central Laboratory)

Mr. Takashi Yabe	(Tokyo Institute of Technology)
Prof. Chiyoe Yamanaka	(Osaka Univ.)
Assoc. Prof. Tatsuhiko Yamanaka	(Nagoya Univ.)
Prof. Masahiro Yokoyama	(Osaka Univ.)

Two-Step Laser-Driven Fusion Reactor

Takashi Yabe

Department of Energy Sciences, Tokyo Institute of Technology, Tokyo, Japan

Katsunobu Nishihara

Department of Physics, Nagoya University, Nagoya, Japan

Jun-ichi Mizui

Institute of Plasma Physics, Nagoya University, Nagoya, Japan

Abstract

We present a new type of laser fusion reactor which consists of a small core pellet and a large outer pellet.

In order to realize the laser-induced thermonuclear fusion reaction in practical sense, we need several tens of operations per second because of its small pellet size and the limitation to the laser power. You can see that these successive operations may become a final and serious trouble for laser fusion.

In this paper, we propose the new type of the fusion reactor. This reactor is consisted of a small "core pellet" covered with a large amount of D-T fuel, which we call the "outer pellet" hereafter. As shown in Fig.1, there is a narrow gap between the core pellet and the outer pellet.

At the first step, we need to deposit the laser energy only to the core pellet, then the core pellet implods and the thermonuclear fusion reaction occurs. If the core pellet completely burns, its energy is estimated to be several thousands times greater than the input laser energy and its output energy drives the fusion wave propagating outward through the outer pellet.

The first problem that we must solve is how we can deposit the laser energy only to the core pellet. Here we have a very simple and fruitful method. We can make tunnels with a small radius obliquely through the outer pellet. These tunnels must be obliquely to the radial direction in order to suppress the backscattering loss. In this configuration, the laser lights which come in through the tunnels experience several reflections between the core and the outer pellets,

and finally lose all their energy without returning back through tunnels. These tunnels play another role on the implosion of the core pellet. A suitable arrangement of tunnels may cause the rotation of the corona of the core pellet. There is the possibility that this corona rotation may stabilize the Rayleigh-Taylor instability , the thermal instability and other instabilities. For example the growth rate of the Rayleigh-Taylor instability with the fluid rotation Ω is

$$\gamma^2 = -2\Omega^2 + \sqrt{4\Omega^4 + g^2k^2} \,. \qquad (1)$$

We must refer to a trivial question about tunnels. Are the tunnels filled up with expanding wall materials and are the laser lights shut out from tunnels before the implosion of the core pellet completes ? The answer is "yes". But we can overcome this difficulty, winding coils inside the walls of tunnels. The magnetic fields induced by these coils suppress the expansion of the wall materials.

The second problem is the propagation of the fusion wave through the outer pellet. Here we calculate the core pellet size needed for the ignition of the fusion wave. At first, let's consider the point explosion where the size of the core pellet is negligibly smaller than that of the outer pellet. At the initial phase of the explosion the thermal conduction is the leading term, so we can assume

$$\frac{\partial T_e}{\partial t} = a \frac{1}{r^2} \frac{\partial}{\partial r} \left(r^2 T_e^{5/2} \frac{\partial T_e}{\partial r} \right), \qquad (2)$$

and

$$Q = \int_0^\infty T_e r^2 \, dr \tag{3}$$

are the governing equations, where

$$a = K_{e0}(2m_i/3k), \quad Q = E_{in}/(6\rho k\pi/m_i), \tag{4}$$

and E_{in} is the energy deposited by the core pellet implosion. The solution of (2) and (3) can be obtained using the transformation

$$T_e = \left(\frac{Q^{2/3}}{at}\right)^{6/19} f(\xi), \tag{5}$$

and the similarity parameter

$$\xi = \frac{r}{(Q^{5/2}\, at)^{2/19}}, \tag{6}$$

where $f(\xi)$ satisfies the following ordinary differential equation

$$\frac{d}{d\xi}\left(f^{5/2}\frac{df}{d\xi}\right) + \left(f^{5/2} + \frac{2}{19}\xi^2\right)\frac{df}{d\xi} + \frac{6}{19}\xi^2 f = 0 \tag{7}$$

Without knowing the solution of eq.(7) we can get some conclusions. The electron temperature decreases with increasing time as $T_e \propto Q^{4/19}\, t^{-6/19}$. The ignition of the fusion wave may be assumed to occur when the ion temperature becomes as high as the electron temperature. At this time t_1,

$$T_e = T_i = T_1 \propto Q^{1/7} \tag{8}$$

where

$$t_1 \propto Q^{3/4}. \tag{9}$$

The ignition condition is

$$W \geq A\rho T_1^{1/2} + \frac{6}{19}\frac{T_1}{t_1}, \tag{10}$$

$$A = (2/3km_i)\times 1.42\times 10^{-27} \quad (K^{1/2}cm^3g^{-1}sec^{-1})$$

where the left hand side of eq.(10) is the fusion reaction, and the right hand side of eq.(10) is the sum of the bremsstrahlung and the thermal conduction loss. These values are plotted in Fig.2 versus the initially deposited energy. The condition (10) is satisfied with $E_{in} = 8\times 10^{13}$erg. This energy should be deposited by the implosion of the core pellet with an initial radius R_0 and density n_0, that is

$$\frac{4}{3}\pi\, n_0\, R_0^3\, E_\alpha = E_{in}, \tag{11}$$

where n_0 is the solid density and E_α the energy of a α-particle. From eq.(11) we get

$$R_0 = 400\ \mu m.$$

As the temperature is 14.1 keV at this condition and the mean free path of α-particles is about 1.6 cm, the outer pellet should have a radius greater than 1.6cm . If we use a outer pellet of 4 cm in radius and do one operation per second, the yield power of α-particles is estimated as 10^6 kW.

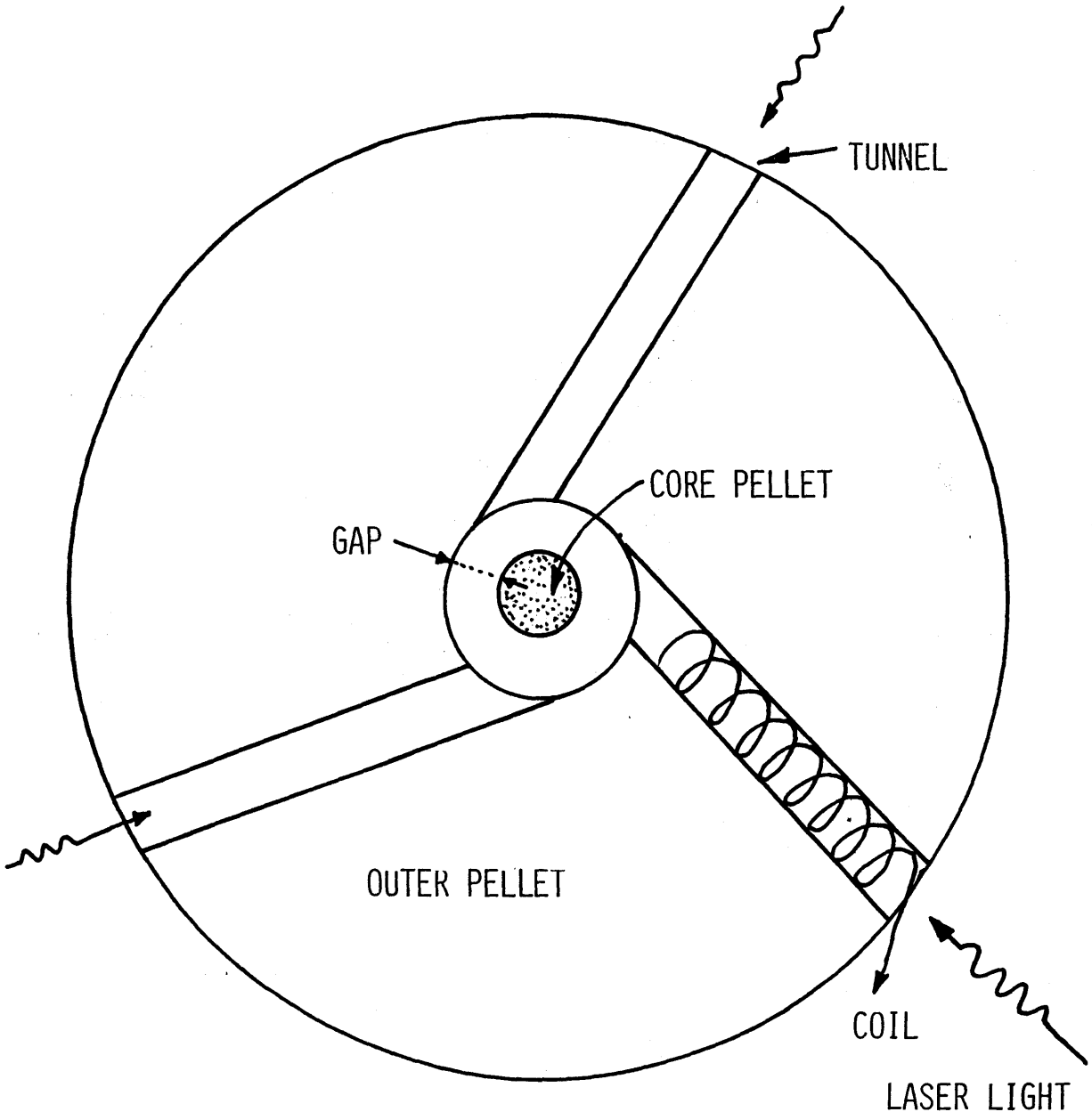

Fig.1 The schema of the fusion reactor.

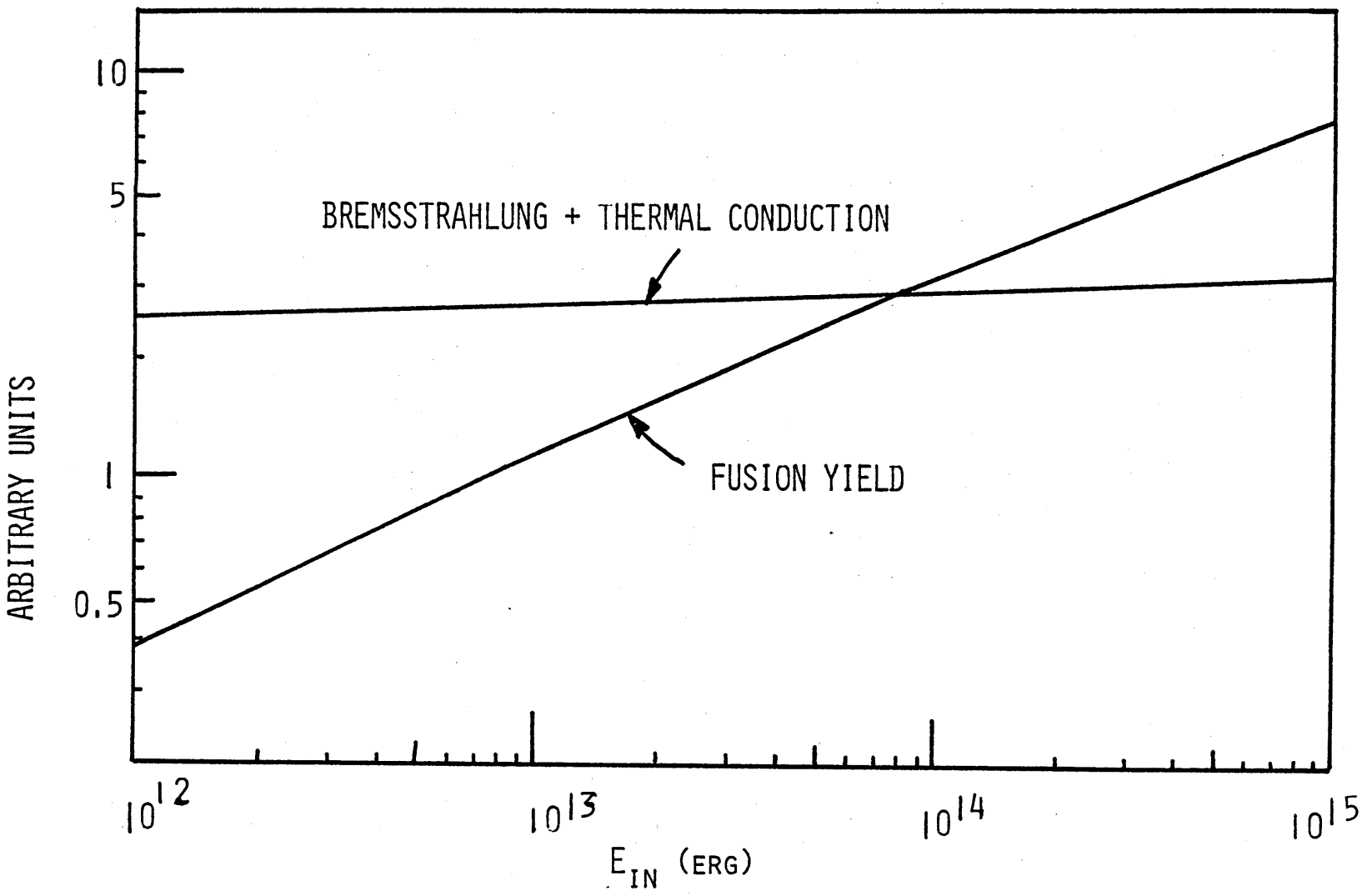

Fig.2 The values of the right hand side and the left hand side of eq.(10).

Filamentation and Decay of Laser Light in Plasmas

Katsunobu Nishihara

Department of Physics, Nagoya University, Nagoya, Japan

Kunioki Mima

Department of Electrical Engineering, Osaka University, Osaka, Japan

Jun-ichi Mizui, Masaaki Inutake

Institute of Plasma Physics, Nagoya University, Nagoya, Japan

Toshio Tange

Department of Physics, Hiroshima University, Hiroshima, Japan

Yasuhito Kiwamoto

Institute of Materials Science and Engineering., Yokohama National University, Yokohama, Japan

Masashi Kako

Plasma Physics Laboratory, Osaka University, Osaka, Japan

Abstract

Filamentation of laser light is studied for a laser fusion plasma. We also discuss the importance of effects of a decay of the laser light into two plasma waves on the filament formation at one-quarter critical density

The production of useful amounts of fusion energy can result only if D-T pellet is highly and effeciently compressed. The pellet compression may, however, be limited by departures from spherical symmetry produced by nonuniformity of laser energy deposition, although large electron thermal conduction alleviates the nonuniformity. Strong filamentation of laser-light can, if it occurs, markedly affect the uniformity of laser deposition. For this reason it seems important to study the formation of filaments of the laser light. We shall first discuss the formation of filaments in a uniform underdense plasma. We have examined this process via an instability analysis. Second, we discuss the importance of effects of a decay of the laser wave into two plasma waves on the filament formation at one-quarter critical density.

We begin with self-focusing of an electromagnetic wave in a uniform underdense plasma with cold ions and warm electrons. Self-focusing of the electromagnetic wave in such a plasma can be described by the following cylindrical symmetry equations,[1]

$$i\left(\frac{1}{\lambda_g}\frac{\partial}{\partial t}+\frac{\partial}{\partial z}\right)E+\frac{1}{2k_0}\frac{1}{r}\frac{\partial}{\partial r}\left(r\frac{\partial}{\partial r}E\right)-\frac{\omega_p^2}{2k_0c^2}\frac{\delta n}{n_o}E=0 \quad . \tag{1a}$$

$$\frac{\delta n}{n_0}=-2\frac{\omega_p^2}{\omega_0^2}\frac{|E|^2}{4\pi n_0 T} \quad , \tag{1b}$$

where n_0 the unperturbed plasma density, δn the perturbed plasma density induced by the ponderamotive force due to the wave, c the light velocity, λ_g the group velocity of the wave, ω_p the electron plasma frequency and T the electron temperature in energy unit. Here, the original wave has been assumed to propagate in the Z direction with the phase $\exp[ik_0z-i\omega_o t]$ and with the amplitude E which slowly

varys with the time t and the space z and r. The wave number k_0 and the frequency ω_0 are also assumed to satisfy the linear dispersion relation,

$$\frac{k_0^2 c^2}{\omega_0^2} = \varepsilon = 1 - \frac{\omega_p^2}{\omega_0^2} \quad . \tag{2}$$

The passage of the intese wave through the plasma can modify the index of refraction in such a way that the wave is focused into a smaller cross section. If the ponderamotive force due to the wave can overcome the plasma thermal pressure, the wave can expel some of the plasma. The wave can then focus further.

We now estimate the e^{-1}-fold distance in cross section of the wave, using the linear instability analysis.[2] To do this we consider a steady propagation of the wave in the z direction and a sinusoidal modulation in the r direction. The spatial growth rate of such a sinusoidal self-focusing can be given by,[2]

$$\gamma = \frac{k_r}{2k_0}\left[\left(\frac{E_0^2}{4\pi n_0 T}\right)\frac{1}{\varepsilon}\frac{\omega_0^2}{c^2} - k_r^2\right]^{1/2} \quad , \tag{3}$$

where k_r is the filamentation wave number in the r direction. $L=\gamma^{-1}$ gives the e-fold distance in the square of the amplitude of the wave, hence the e^{-1}-fold distance in its cross section.

$L \sim 50$ μm in the case of the typical laser beam, $E_0^2/4\pi n_0 T \sim 10^{-1}$, $k_0 \sim 2\pi \times 10^{-4}$ μm^{-1} and $k_r \sim \pi \times 10^{-1}$ μm^{-1}. Here, we have assumed $\omega_p^2 << \omega_0^2$, and $a=2\pi/k_r$ has been taken to be the radius of the typical laser beam, $a \sim 20$ μm, although the assumption of the sinusoidal modulation in the r direction is not valid. Since the typical length of the expanding underdense plasma is of order

100 μm, the effect of the self-focusing of the whole laser beam can be ignored.

At intensities well above threshold for self-focusing the beam breaks up into filaments. The filamentation can become important, as shown below. The spatial growth rate vanishes at $k_r=0$ and at large k_r, where the ponderamotive force can no longer exceed the plasma pressure. The growth rate has a maximum at $k_{r_{max}}=E_0^2\omega_0^2/8\pi nTc^2$. In the case $E_0^2/4\pi n_0 T \sim 10^{-1}$ and $k_0 \sim 2\pi \times 10^{-4}$ μm^{-1}, the minimum e-fold length becomes $L \sim 10$ μm at $a=2\pi/k_{r_{max}} \sim 4$ μm. The filamentation with the small radius can then be dangerous in the formation of the uniform laser energy deposition.

The above results are, however, necessarily inconclusive since we have assumed the sinusoidal modulation in the r direction. For the actual modulation of the laser beam, it is desirable to solve eq.(1) exactly. Also, as we shall discuss below, eq.(1) itself does not hold in the whole underdense region.

We now consider effects of decay instabilities of the electromagnetic wave on the filament formation at one-quarter critical density. When $\omega_0 \sim 2\omega_p$, the wave decays into two plasma waves ("$2\omega_p$" instability) or a plasma wave and a scattered electromagnetic wave (stimulated Raman scattering). Stimulated Raman scattering may not markedly affect the filament formation of the wave, because the decay waves propagate in the same direction of the original wave. The decay plasma waves associated with the $2\omega_p$ instability can, as we show below, give rise to the larger density perturbation propagating in the direction of the electric field of the laser wave. The decay plasma waves can then affect the filament formation.

When the wave number of the decay plasma wave k' is large and satisfies the inequality $k'\lambda_0 > (m/M)^{1/2}$, where λ_0 is the electron debye length, and m and M are respectively the electron and ion masses, the decay plasma wave can excite an ion acoustic wave due to a decay instability, a decay of the plasma wave into an ion acoustic wave and a backward plasma wave. The amplitude of the excited wave in the decay instability is proportional to that of the pump wave. The plasma density perturbation associated with the excited ion wave can then be of the first order in the amplitude of the electric field of the laser wave. As we have shown in eq.(1b), the plasma density expelled by the laser wave is, however, of the second order in the amplitude the electric field. The density perturbation due to the decay plasma wave can thus modify the index of refraction for the laser wave.

When $k'\lambda_0 \gtrsim (m/M)^{1/2}$, the decay plasma waves are modulationally unstable. The ponderamotive force associated with the decay plasma wave induces the plasma density perturbation. The density perturbation becomes of the first order in the amplitude of the decay wave, hence of the first order in that of the laser wave, provided $k'\lambda_0 \sim (m/M)^{1/2}$. The density perturbation due to the modulational instability can then also modify the index of refraction.

In both cases, the crucial point is that the induced density perturbations are large and can propagate out in the radial direction with an ion acoustic speed even in the existence of the density gradient.

References

1. See, for a example, P. Kaw, G. Schmidt and T. Wilcox, Phys. Fluids 16, 1522 (1973).

2. A. B. Langdon and B.F. Lasinski, Phys. Rev. Let. 34, 934 (1975).

Magnetic Field Generation Due to Resonance Absorption

Katsunobu Nishihara, Yukiharu Ohsawa
Department of Physics, Nagoya University, Nagoya, Japan

Kunioki Mima
Department of Electrical Engineering, Osaka University,
Osaka, Japan

Toshio Tange
Department of Physics, Hiroshima University, Hiroshima, Japan

Abstract

A detailed study of mechanism of megagauss magnetic field generation in resonant absorption of laser light is presented which takes into account effects of both dissipation and thermal motion of electrons.

Recently strong magnetic fields have been observed in laser-produced plasmas.[1,2] The occurance of the strong magnetic field can affect plasma behavior through hydrodynamic effects or from alternations of the plasma transport coefficients.[3] It is thus important to study the mechanism of the magnetic field generation in laser-produced plasmas. Most theoretical work has been done for the field due to the thermoelectric current,[2,4] while investigation of the field derived from the radiation pressure have been either incomplete or incorrect.[5]

We present here a mechanism of the magnetic field generation which is inherent in resonant absorption. When laser light is obliquely incident on a warm plasma with a density gradient and polarized in the plane of incidence, it can be absorbed resonantly by linear mode conversion into an electron plasma wave.[6,7] At high intensities a large dissipation has been observed in computer experiments.[8] The dissipation then gives rise to a phase lag between the electron oscillatory motion and the wave, which can introduce a time-averaged force on the electrons, hence an electron current. The thermal motion of the electrons allows the propagation of the resonantly excited plasma wave along the density gradient.[9] The nonlinear interaction between the light wave and the plasma wave can also set up an additional electron current. The currents can give rise to a magnetic field of the order of a megagauss.

The analysis can be carried out to a first approximation by use of the equation of motion for the electrons

$$\left(\frac{\partial}{\partial t} + \underset{\sim}{v}\cdot\nabla\right)\underset{\sim}{v} = -\frac{e}{m}\left(\underset{\sim}{E} + \frac{1}{c}\underset{\sim}{v}\times\underset{\sim}{B}\right) - \frac{1}{mn}\nabla p - \nu\underset{\sim}{v} \qquad (1)$$

and Maxwell's equations, where ν is the effective collision frequency and others are in standard notations. We consider two time scales, the time ω^{-1} corresponding to the laser light, and the time associated with the fluid dynamics. The high frequency parts can be described by the sets of the linearized equations. Under the assumption that the fields vary with the time as $\exp(-i\omega t)$, the oscillating velocity $\underset{\sim}{v}'$ can be obtained as

$$\underset{\sim}{v}' = -i \frac{1}{\omega+i\nu}\left[\frac{e}{m}\underset{\sim}{E}' + \frac{T}{4\pi e m n_0}\left\{(\underset{\sim}{\nabla}\cdot\underset{\sim}{E}')\frac{\underset{\sim}{\nabla} n_0}{n_0} - \gamma\underset{\sim}{\nabla}(\underset{\sim}{\nabla}\cdot\underset{\sim}{E}')\right\}\right] \quad , \quad (2a)$$

where the oscillating electric field $\underset{\sim}{E}'$ satisfies the wave equation[8]

$$\nabla^2\underset{\sim}{E}' - \underset{\sim}{\nabla}(\underset{\sim}{\nabla}\cdot\underset{\sim}{E}') + \left(\frac{\omega}{c}\right)^2\left(1 - \frac{\omega_p^2}{\omega(\omega+i\nu)}\right)\underset{\sim}{E}' + \left(\frac{\omega}{c}\right)^2 \frac{T}{m\omega(\omega+i\nu)}\Big\}\gamma\underset{\sim}{\nabla}(\underset{\sim}{\nabla}\cdot\underset{\sim}{E}')$$

$$- (\underset{\sim}{\nabla}\cdot\underset{\sim}{E}')\frac{\underset{\sim}{\nabla} n_0}{n_0}\Big\} = 0 \quad , \quad (2b)$$

where n_0, T and ω_p are the background plasma density, the electron's temperature and the local electron plasma frequency, respectively, and γ is the ratio of specific heats. Here we have assumed an adiabatic pressure law for high-frequency electron motion and the homogeneous electron temperature.

Taking the average of the equation of motion for the electrons, Eq. (1), over a period $2\pi\omega^{-1}$, we can get the equation for the induced electric field $\underset{\sim}{E}_0$ slowly varying with time as

$$\langle(\underset{\sim}{v}'\cdot\underset{\sim}{\nabla})\underset{\sim}{v}'\rangle = -\frac{e}{m}\left(\underset{\sim}{E}_0 + \frac{1}{c}\langle\underset{\sim}{v}' \times \underset{\sim}{B}'\rangle\right) + \frac{\gamma T}{m n_0^2}\langle n'\underset{\sim}{\nabla} n'\rangle \quad , \quad (3a)$$

where $\underset{\sim}{B}'$ and n' are the oscillating parts of the magnetic field

and the electron density perturbation, respectively. Farady's law then gives the rate of increase of the induced magnetic field $\underset{\sim}{B}_0$ as

$$\frac{\partial \underset{\sim}{B}_0}{\partial t} = -c\underset{\sim}{\nabla} \times \underset{\sim}{E}_0 \quad . \tag{3b}$$

To describe the correct time evolution of the slowly varying fields, one has to to take into account the slow motion of both the electrons and the ions. Since the purpose of the present analysis is, however, to explain the mechanism of a megagauss field generation, we do not here consider the fluid dynamics. Substituting Eqs.(2a) and (3a) into Eq.(3b) and neglecting the terms proportional to ν^2/ω^2, $(\nu/\omega)(k^2T/m\omega_p^2)$ and $(k^2T/m\omega_p^2)^2$, we can obtain the equation for the induced magnetic field $\underset{\sim}{B}_0$ in terms of the electric field $\underset{\sim}{E}'$ as

$$\frac{\partial \underset{\sim}{B}_0}{\partial t} = -\frac{c}{\omega^2}\left(\frac{e}{m}\right)\underset{\sim}{\nabla} \times \left[\underset{\sim}{E}' \times \left\{ i\frac{\nu}{\omega}\underset{\sim}{\nabla} \times \underset{\sim}{E}^* + \frac{(\gamma-1)T}{\omega_p^2 m}\frac{\underset{\sim}{\nabla} n_0}{n_0} \times \underset{\sim}{\nabla}(\underset{\sim}{\nabla}\cdot\underset{\sim}{E}^*)\right\}\right.$$

$$\left. + \text{c.c.}\right] \quad , \tag{4a}$$

where the adscript * denotes the complex conjugate. Solving the wave equation (2b) under the appropriate boundary condition, and using the obtained electric field, one can calculate the time rate of increase of the magnetic field. It is now guite obvious that the radiation pressure can induce the magnetic field only if either the dissipation or the thermal motion is present. It is also noted that the term due to the dissipation does not depend on the density gradient n_0 explicitly, although it

determines the shape of the electric field $\underset{\sim}{E}'$ through the wave equation (2b).

We now consider the specific case of a slab of plasma with $n_0=n_0(z)$ and the electromagnetic wave obliquely incident on this slab, with the electric field polarized in the plane of incidence, the y-z plane. The y dependence of the field can be assumed to be periodic in y and of the form $\exp(ik_y y)$. In this case, Eq.(4a) can be written in the form

$$\frac{\partial B_{0x}}{\partial t} = \frac{c}{\omega^2}\left(\frac{e}{m}\right)\frac{\partial}{\partial z}\left[E_z\left\{\frac{\nu}{\omega}\left(k_y E_z^* - i\frac{\partial}{\partial z}E_y^*\right)\right.\right.$$

$$\left.\left. + ik_y\frac{(\gamma-1)T/m}{\omega_p^2}\left(\frac{\partial}{\partial z}E_z^* - ik_y E_y^*\right)\frac{\partial}{\partial z}\ln n_0\right\} + \text{c.c.}\right] . \tag{4b}$$

The magnetic field source is zero if there is no electric field component in the direction of the density gradient. The resultant field is thus inherent in the oblique incidence of laser light. It should be emphasized that the induced magnetic field is polarized perpendicular to the axis of light incidence in contrast with that due to the thermoelectric current, which is doughnut shaped. Thus, the magnetic field discussed here can markedly affect the plasma behavior at near the resonant absorption region.

To estimate the rate of increase of the magnetic field, we assume a linear density profile, $n_0(z)=n_c(1+z/L)$, where $\omega_p(z=0)=\omega$ and $\omega L/c \gg 1$. With the aid of the well known solution of Eq.(2b),[7,9] the rate of increase of the magnetic field can approximately become

$$\frac{\partial B_{0x}}{\partial t} \simeq 16\left(\frac{e}{mc}\right)\left(\frac{E_0^2}{8\pi}\right)\exp\left(-\frac{4}{3}k_0 L\sin^3\theta\right)\left[\frac{\nu}{\omega k_0^2 L^2\sin^2\theta}\left(\xi^{-2}+\text{c.c.}\right)\right.$$

$$+ 2\sqrt{\pi}\sin^3\theta\left(\frac{\lambda_D}{L}\right)^{1/2} \xi^{1/4} \ln(k_o L\xi\sin\theta) \cos\left(\frac{2L}{3\lambda_D}\xi^{3/2} + \frac{\pi}{4}\right)] \quad , \tag{5}$$

in the vicinity of the critical density, where E_0, k_0, θ and λ_D are the amplitude of the incident electric field, its wave number, the angle of incidence and the electrons debye length at the critical density, respectively, and $\xi=-z/L-i(\nu/\omega)$. Equation (5) is valid only for $(\lambda_D/L)^{2/3} \lesssim |z/L| < \sin\theta$. At low intensity and very close to the critical density, the effective collision frequency can be approximated by convection loss of plasma wave as $\nu/\omega \sim (\lambda_D/L)^{2/3}$.[9] If this is the case and for a plasma produced by a Nd glass laser with an intensity 10^{15}W/cm^2 and $L \sim 10^{-2}$cm, $T \sim 300$ eV and $\theta \sim 5^o$, as an example, Eq.(5) predicts $\partial B/\partial t \sim 10$ megagauss/psec at near the critical density. In this case, the magnetic field is mostly due to the dissipation effect, i.e. the first term in Eq.(5). At high intensity, however, the large dissipation has been observed of the order of $\nu/\omega \sim 10^{-1}$ in computer experiments.[8] Using this effective collision frequency with the same parameters, we find that $\partial B/\partial t \sim 100$ kilogauss/psec and that the magnetic fields due to the dissipation and the thermal effects are the same order of the magnitude. In the region close to the critical density, the dissipation effect is dominant and the spatial profile of the magnetic field is proportional to $\sim |z|^{-2}$ provided $|z/L| \gtrsim (\lambda_D/L)^{2/3}$. The thermal effect can become important in the region away from the critical density, and the magnetic field can then start to oscillate in space with the wavelength of the order of $\lambda_D(L/\lambda_D)^{1/3}$.

So far, we did not consider the slow motion of the plasma. The electrons are, however, expelled away by the force described in Eq.(3a), as the resonantly excited waves grow. The resultant current in the negative z-direction can then limit the growth of the magnetic field. This current was also observed in the computer experiments.[8] The steady state can be thus reached when $B_{0x} \sim -E_{0y}/v_{0z}$. Here E_{0y} is the solution of the y component of Eq.(3a). v_{0z} can be taken to be c_s at minimum in the order of the magnitude, since otherwise the electron motion gives rise to the ion motion. Under these assumptions with the same parameters used above, we obtain $B_{0max} \sim 10$ megagauss.

Both the dissipation and the thermal motion of the electrons have been shown to introduce megagauss magnetic field at near the resonant absorption region, which is polarized perpendicular to the axis of light incidence. Thus, the magnetic field can markedly affect the plasma behavior at the critical density. The spatial profile of the magnetic field have been also discussed for the slab of plasma with the linear density profile. For laser fusion plasma, the hydrodynamic motion of the plasma modifies the density profile and hence the shape and amplitude of the magnetic field.

This work was initiated at the laser fusion workshop held at Mt. Daisen in Tottori prefecture, Japan. The authors appreciate financial support by Prof. Chiyoe Yamanaka for the workshop. We would also like to thank Dr. Akira Hasegawa for valuable discussions.

References

1. J.A. Stamper and B.H. Ripin, Phys. Rev. Lett. 20, 138 (1975); F. Schwirzke and L.L. Mckee, in Proceedings of the Fifth European Conference on Controlled Fusion and Plasma Physics, Grenoble, France, 1972.
2. J.A. Stamper, K. Papadopoulos, R.N. Sudan, S.O. Dean, E.A. McLean, and J.M. Dawson, Phys. Rev. Lett. 26, 1012 (1971).
3. J.B. Chase, J.M. LeBlanc, and J.R. Wilson, Phys. Fluids 16, 1142 (1973); N.K. Winsor and D.A. Tidman, Phys. Rev. Lett. 31, 1044 (1973).
4. D.A. Tidman and R.A. Shanny, Phys. Fluids 17, 1207 (1974).
5. J.A. Stamper and D.A. Tidman, Phys. Fluids 16, 2024 (1973); J.J. Thompson, C.E. Max, and K. Estarbrook, UCRL Report No. 76690 (submitted for Phys. Rev. Lett.).
6. J.P. Freidberg, R.W. Mitchell, R.L. Morse, and L.L. Rudsinski, Phys. Rev. Lett. 27, 795 (1972).
7. V.L. Ginzburg, Propagation of Electromagnetic Waves in Plasmas (Pergamon, N.Y., 1970), Section 20.
8. D.W. Forslund, J.M. Kindel, Kenneth Lee, E.L. Lindman, and R.L. Morse, Phys. Rev. A11, 679 (1975).
9. V.B. Gil'denberg, Zh. Eksp. Teor. Fiz. 45, 1978 (1963) [Sov. Phys. — JETP 18, 1359 (1964)].

A DESIGN OF STEADY STATE FUSION BURNER

by

Akira Hasegawa
Bell Laboratories, Murray Hill, New Jersey,
07974, U.S.A., and Institute of Plasma Physics
Nagoya University, Nagoya Japan

Tadatsugu Hatori
Institute of Plasma Physics,
Nagoya University
Nagoya Japan

Kimitaka Itoh
Department of Physics,
University of Tokyo,
Tokyo Japan

Takashi Ikuta, Yuji Kodama
and Kazuhiro Nozaki
Department of Physics,
Nagoya Japan

ABSTRACT

We present a brief design of a steady state fusion burner in which a continuous burning of nuclear fuel may be achieved with output power of a gigawatt. The laser fusion is proposed to ignite the fuel.

I. INTRODUCTION

Primary goal of the recent research on the thermo-nuclear fusion is to achieve a break even in the fusion energy output as compared with the input thermal energy to the plasma. Consequently, both the magnetic and the inertia confinement schemes seem to have a problem in future to produce reasonably large power output to compensate the enormous initial construction cost. For example, to achieve 1 GW power station using a Tokamak, in which the density and containment time is limited to 10^{14} and 1 sec respectively, one needs a plasma volume of approximately 10^3 m^3. In case of the inertia confinement scheme using laser(s) 1 GW output is achieved by firing 100 lasers with 10 kJ each 10 times per second even if the energy multiplication fact is taken to be 100.

To overcome these difficulties we have searched for a simple structure with a reasonable set of design parameters

for a continuously operated fusion reactor having 1 GW output power. A simple structure of this type of machine is a magnetically confined long linear machine, in which the fuel is injected from one end of the machine. The brief sketch is shown in Fig. 1.

As the fuel moves toward the right (output side), it changes to a plasma and is heated by the α particles which are self-generated by the fusion. A multi-mirror system is considered to reduce the size of the machine, but if it proves to be unstable, it can be replaced by a longer linear machine of a size of about 7 km to achieve the Lawson criterion for the same temperature.

A linear machine is considered (1) for the simplicity of the structure, thus is accessible to a high β situation, (2) and for the feasibility of a continuous operation.

In Section II we obtain the temperature and density profile under a stationary operation condition and in Section III we show some nominal operation parameters. One typical set of parameters we find is length; 1 km (multi-mirror), density and temperature at output side; 2×10^{16} cm^{-3}, and 5 keV, flow speed at the output side; 4×10^{4} m/s, α particle output power; 6×10^{8} W/m^{3}.

II. PROFILE OF PLASMA PARAMETERS FOR A STATIONARY OPERATION

Here we obtain the spatial profile of plasma parameters for which a stationary burner operation is feasible. The stationary profile is achieved (1) by the balance of the pressure gradient and the flow velocity gradient and (2) by the balance of the heat flow and the thermal conduction plus the α particle heating. If we ignore the perpendicular loss,[1] the stationary profile along the magnetic field of the thermodynamic quantities obeys, the equation of continuity,

$$nv = \text{constant } (= J_o) , \tag{1}$$

the equation of motion,

$$nm_i \frac{v^2}{2} + nT = \text{constant } (= \pi_o), \tag{2}$$

and the equation of heat flow

$$\frac{\partial}{\partial x} \left(nvT - \kappa \frac{\partial T}{\partial x} \right) = S . \tag{3}$$

In these expressions, v is the flow speed, n the plasma density, T the temperature ($T_e = T_i$ is assumed for a density of $\sim 10^{16}$ cm^{-3}), m_i the ion mass κ the heat conductivity and S is the heat source due to the α particle

heating, which is given by

$$S = n_\alpha W_\alpha \frac{m_e}{m_\alpha} \nu_e \tag{4}$$

with

$$\nu_e = \frac{\omega_{pe}}{n\lambda_D^3} \frac{\ell n \Lambda}{3\pi\sqrt{\pi}} \quad . \tag{5}$$

In Eqs. (4) and (5) n_α, W_α, m_α are the density, kinetic energy (3.5 MeV) and mass of the α particle, ω_{pe}, λ_D, and $\ell n \Lambda$ are the electron plasma frequency, the Debye wavelength and the Coulomb logarithm. For the heat conductivity κ, we should use the electron heat conductivity κ_e for a linear machine,

$$\kappa_e (ms)^{-1} = 2.6 \times 10^{22} \, T^{5/2} \quad (eV), \tag{6}$$

while for a multi-mirror, because the electrons move only with the ions, the ion heat conductivity κ_i may be used,[2]

$$\kappa_i (ms)^{-1} = 5.2 \times 10^{20} \, T^{5/2} \quad (eV). \tag{7}$$

Equations (1) to (3) are valid of course, only in the region after the incident gas is ionized. For simplicity we do not consider the ionization stage. We also assume D-T fusion here.

From Eqs. (1) and (2) we can immediately obtain the relation between n, v and T. If we assume $T >> \frac{1}{2} mv^2$

and use subscript I and II to denote quantities at the input (after ionization) and output. Then

$$v(x) = \frac{T_I - \sqrt{T_I^2 - 2m_i v_I^2 T(x)}}{m_i v_I^2} \quad . \tag{8}$$

A stationary condition is obtained only when

$$T_{II} < \frac{T_I^2}{2m_i v_I^2} \quad , \tag{9}$$

which will be found to be satisfied for our choice of parameters later. If we assume $T_{II} \ll T_I^2/(2m_i v_I^2)$, we have

$$\frac{v(x)}{v_I} = \frac{T(x)}{T_I} \quad , \tag{10}$$

and

$$\frac{n(x)}{n_I} = \frac{T_I}{T(x)} \quad . \tag{11}$$

To obtain the explicit profile of these quantities as a function of distance x, we must integrate Eq. (3). However because of the T dependency of κ and S, the explicit form cannot be obtained by a simple function. Hence we solve Eq. (3) piecewise. First, close to the output side where

the α particle heating may be less effective due to the smaller collision frequency, we ignore S and obtain

$$T = T_{II} \left(\frac{5x}{2L_c} \right)^{2/5} , \tag{12}$$

where L_c is the characteristic distance decided by the normalized thermal conductivity $\bar{\kappa}$ given by

$$L_c = \frac{\bar{\kappa}}{J_o} , \tag{13}$$

and

$$\bar{\kappa} = \kappa \left(\frac{T_{II}}{T} \right)^{5/2} . \tag{14}$$

Second, in the intermediate region where the α particle heating dominates over the thermal conduction due to the higher density and lower temperature, the temperature profile becomes

$$T = T_{III} \left(\frac{7x}{2L_\alpha} \right)^{2/7} , \tag{15}$$

where T_{III} is the appropriate temperature which connects to the region given by Eq. (12), and L_α is the characteristic distance decided by the α particle heating

$$L_\alpha = \frac{J_o T_{III}}{S_{III}} . \tag{16}$$

S_{III} is the normalized heat source given by

$$S_{III} = S \left(\frac{T_{III}}{T} \right)^{-5/2} . \qquad (17)$$

In the derivation of Eq. (15), a constant density for α particles is assumed.

These solutions give a relatively weak dependency on x.

III. SOME DESIGN PARAMETERS

In this section, we present conditions that the stationary burning are achieved (Lawson criterion for the burner) and show some concrete examples for the choice of the design parameters.

As the fundamental relation for the design parameters, we use the scale size L_c as the measure of the machine length,

$$L \equiv L_c = \frac{\kappa}{J_o} , \qquad (13)$$

with κ given by the output temperature. If we assume the use of a multi-mirror system, we may use the ion thermal conductivity. Then Eq. (13) can be written

$$L(m)n(m^{-3})v(m/s) = 1.34 \times 10^{28}\ T^{5/2}\ (keV), \qquad (13')$$

where all the quantities are those at the output end and are expressed in terms of MKS units, except for T which has a unit of keV.

The Lawson criterion in this case is given by the condition that the power loss from the output side nTvS is smaller than the power generation by the α particle of the fusion product. Here S is the cross sectional area of the machine. A minimum size of the cross section may be decided by the Larmor radius of the α particle. For a 100 kG magnetic field, this Larmor radius is 4 cm. Hence a radius of 8 cm may be a good minimum choice for the cross section of the machine. For this choice $S = 2\times10^{-2}\ m^2$.

The Lawson criterion is given by

$$n(m^{-3})v(m/s)T(keV)S(m^2)$$

$$< 3.22\times10^{-15}\ L\ (m)\ n^2\ (m^{-3})S(m^2)\ T^{-2/3}\ (keV)\ \exp\left[-20\ T^{-1/3}(ke\right.$$

(18)

We use Eq. (9) as a subsidiary condition that the choice of the parameter should satisfy. We choose $T_I \sim 3$ eV for this purpose.

If we eliminate v from Eq. (13') and (18), we have the condition for Ln

$$Ln > 2.04\times10^{21}\ T^{25/12}\ \exp(10\ T^{-1/3}). \qquad (19)$$

The flow speed v(m/s) at the output end is

$$v = 6.57\times10^{6}\ T^{5/12}\ \exp(-10\ T^{-1/3})\ . \qquad (20)$$

The output power P(w) is given by

$$P = 5.15\times10^{-31}\, S(m^2)L(m)n^2(m^{-3})T^{-2/3}\ (keV)\ \exp\left[-20\ T^{-1/3}\ (keV)\right]$$

$$= 2.14\times10^{12}\ T^{7/2}\ (keV)S(m^2)/L(m). \qquad (21)$$

Note here that because Ln is proportional to $\kappa^{1/2}$, even if a straight machine is assumed in which the electron thermal conductivity operates, the length is increased only by a factor of $(m_i/m_e)^{1/4} \sim 7$. Equations (19), (20), and (21), show the relations among the flow speed v, output temperature and density, T and n, length and the cross sectional area L and S and the output power of α particles P.

If we choose, for example, $L = 10^3$ m, $S = 2\times10^{-2}$ m^2, other quantities are given only by one parameter, the output temperature T. If we take T = 5 keV, we have

$$n = 2\times10^{22}\ m^{-3}$$
$$v = 3.7\times10^{4}\ m/s$$
$$P_\alpha = 1.2\times10^{10}\ W,$$

while for the choice of 4 keV for T,

$$n = 2\times10^{22}\ m^{-3}$$
$$v = 2.14\times10^{4}\ m/s$$
$$P_\alpha = 5.5\times10^{9}\ W.$$

T = 4 keV is just about the temperature at which the Bremsstrahlung loss becomes larger than the fusion power generation.[3] Thus to consider a lower temperature is meaningless. On the other hand if the temperature is increased by a factor of two the output power becomes unrealistically large, unless the length is increased to, say, 10 km.

If a straight machine is used, by replacing the ion thermal conductivity by the electron thermal conductivity in Eq. (13), we have the following set of design equations

$$Ln > 1.6\times10^{22}\ T^{25/12}\ \exp\ (10\ T^{-1/3})\ , \qquad (19')$$

$$v = 5.14\times10^{7}\ T^{5/12}\ \exp\ (-10\ T^{-1/3})\ , \qquad (20')$$

and the corresponding output power becomes

$$P_{\alpha}(W) = 1.32\times10^{14}\ T^{7/2}\ (keV)S(m^2)/L(m)\ . \qquad (21')$$

The nominal values for the parameters for a choice of L = 10 km and T = 5 keV are:

$$n = 1.6\times10^{22}\ m^{-3}$$

$$v = 2.9\times10^{5}\ m/s$$

$$P_{\alpha} = 7.4\times10^{10}\ W.$$

Unfortunately the output power becomes too large in this case.

It should, however, be noticed that these values are the pessimistic side of the estimate, because we have used parameters at the output end. If the realistic temperature profile is used by solving Eq. (13) exactly, it is expected that the length is shortened by a factor of probably five and the output power is reduced by more than a factor of ten.

IV. CONCLUDING REMARKS

We have presented a very brief yet fundamental design parameters for a linear fusion burner. In principle the machine can generate continuous power output of the order of 1 GW. However several unsolved problems still remain. One significant problem is the stability of the plasma as well as that of the plasma flow. Because the loss across the magnetic field is assumed negligible, a plasma instability such as the drift wave mode should be suppressed to the level that the perpendicular diffusion time be smaller than $L/v \sim 0.1$ sec. Also to achieve the stationary burning, temperature and flow speed should be controlled as to meet the stationary solution obtained here. We did not check the stability of our solution and it could very well be unstable under certain circumstances.

The other significant problem is the way to ignite the fuel. We propose to use lasers and DT pellet. For the ignition, one must provide with approximately 10^8 Joule of energy within a tenth of a second. This may be achieved

by a hundred 10 KJ lasers and burning about 10% of the pellet fuel (energy multiplication factor of 100). Because once the ignition takes place, it burns continuously, this scheme gives a greater advantage over the ordinary laser fusion.

It is also worth pointing out that the output side should be covered by a gas blanket for a linear machine to provide enough pressure toward the plasma so that the end loss is not enhanced. The plasma pressure is on the order of 10 to 100 atmospheric pressure.

The overall stable operation of this type of machine may be very delicate. One merit however is that the flow speed is rather low and may be dynamically controlled.

Finally we compare the present proposal with the more well known linear machine concepts.[4] First the present machine aims a complete steady state operation while others are either pulsed or semi-steady state. Second, the energy containment time of the present concept depends on a steady state pressure balance while others on a free flow of ions along the magnetic field which makes the difference in the energy containment time by a factor of v_{Ti}/v favorable to our scheme, where v_{Ti} is the ion thermal speed and v is the steady flow speed of our plasma.

Because of the latter reason, the present machine has in general a shorter length than the other

linear machine for the same nT product. On the other hand because the entire machine should be pressurized, the present concept depends its maximum density on the high pressure technology available in future.

For example if a hundred atmospheric pressure is assumed, the density is limited to 10^{16} cm^{-3} for $T \sim 10$ keV. Another interesting contrast is, because the containment time is limited by the heat conductivity, the present scheme has a power output inversely proportional to the machine length as seen in Eq. (21), which can either be favorable or unfavorable depending on a specific situation.

This work was done during the laser fusion workshop held at Mt. Daisen in Tottori prefecture, Japan. The authors appreciate financial support by Prof. Chiyoe Yamanaka for the workshop. We would also like to thank Prof. Tosiya Taniuti for valuable discussions. Conversations with Dr. Solomon, J. Buchsbaum, Prof. John Dawson, Prof. Allen J. Lichtenberg and Dr. Fred Ribe are greatly helpful.

One of the authors (A.H.) is supported partially by NSF grant #IOP74-12932 during his stay at the Institute of Plasma Physics, Nagoya University.

REFERENCES

1. We assume a magnetic field of about 100 kG and the maximum temperature of the plasma of 5 keV with plasma radius of 10 cm or larger. Then the ratios of the ion Larmor radius to the plasma radius becomes $\lesssim 10^{-2}$.
2. See for example, A. Makhijani, A J. Lichtenberg, M. A. Lieberman and B. G. Logan, Physics of Fluids 17, 1291 (1974).
3. S. Glasstone and R. H. Lovberg, Controlled Thermonuclear Reactors, D. Van Nostrant Co., Princeton, N.J., (1960) p. 35.
4. W. R. Ellis, Nuclear Fusion 15, 255 (1975).

FIGURE CAPTION

Figure 1. Schematical diagram of the proposed fusion burner with a multi-mirror. A continuous operation with output power of 1 GW is feasible with a carefully adjusted flow speed of the plasma, density and temperature profiles. If a straight magnetic field is used, the length and the output power, for a similar set of parameters, becomes approximately ten times.

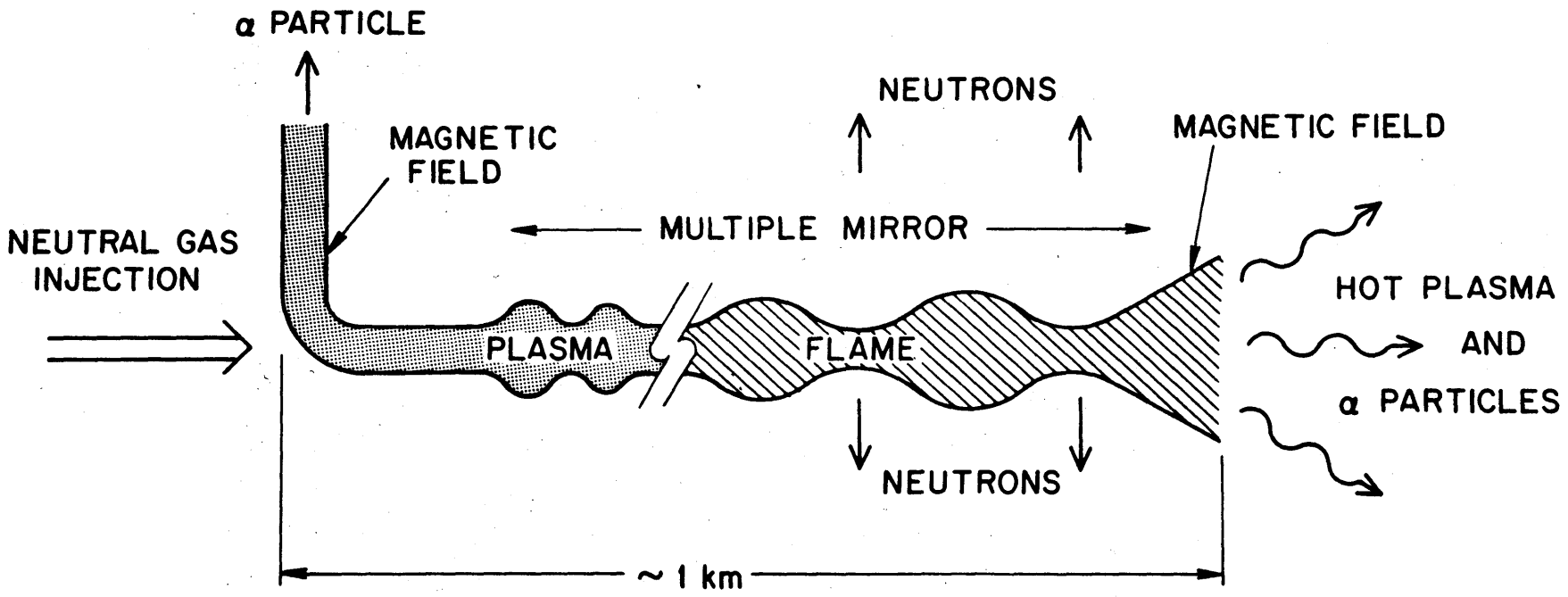
α PARTICLE
NEUTRONS
MAGNETIC FIELD
MAGNETIC FIELD
NEUTRAL GAS INJECTION
MULTIPLE MIRROR
HOT PLASMA AND α PARTICLES
PLASMA
FLAME
NEUTRONS
~ 1 km

MAGNETICALLY FOCUSED FAST ION IN LASER TARGET PLASMA

Kimitaka ITOH and Sanae INOUE

Department of Physics, Faculty of Science, University of Tokyo,
Tokyo, Japan

ABSTRACT

Fast ion generation in the laser target plasma is investigated including the effect of strong magnetic field. Hot electron generates electric field parallel to the laser light and azimuthal magnetic field. A meandering duct, in which ions are accelerated along the magnetic null line, appears in this configuration. Outside the duct $\vec{E} \times \vec{B}$ and $\vec{B} \times \nabla \vec{B}$ drifts play main roles. It is shown that the ion focusing process depends on the direction of the magnetic field.

It is well known that fast ions are emitted from a laser target plasma. The energy of the ions exceeds several 10keV and the beam is broadly focused to the laser. This high energy ion production is not only a phonomenon of physical interest but also a very important probrem from the view point of the Thermo-Nuclear-Fusion-Research, since almost a half of the absorbed energy is carried out by the fast ion from the target. It has been suggested that the fast ion are accelerated by the electric field generated by a hot electron tail [1]. On the other hand, several MG magnetic field is obserbed and is considered to be generated by the hot electron tail too. So it is necessary to include the effect of the magnetic field for a selfconsistent analysis. We present here a model of focused ion acceleration along the magnetic null line in the absence of a turbulence.

When the surface of the target is heated by the laser light, there appears a hot spot of coronal plasma. In the spot, the electron distribution becomes two components. By virture of the reduced thermal conductivity, the diffusion of the hot electron tail is suppressed and its spatial distribution may be taken to be static in the first approximation. Since we intend to show the physical picture of the phenomena, here we use the fluid equations for hot electron and the equation of motion for ion.

In the absence of instabilities the system naturally has

a cylindrical symmetry. We use cylindrical coordinates taking the z axis along the laser beam out of the plasma (Fig.1). We assume that the hot electron is in the stationary state and its pressure gradient is sustained by the ambipolar electric field,

$$en_h\vec{E} + \nabla p_h = 0. \tag{1}$$

The subscript h denotes hot electron. The equation of motion for the ion is

$$M\dot{\vec{V}} = Ze(\vec{E} + \vec{V}\times\vec{B}), \tag{2}$$

(M and Z are mass and charge of an ion respectively). From the cylindrical symmetry, angular momentum $L \equiv Mrv_\theta$ is conserved. The equation of state for the hot electron is $p_h = n_h T_h$. Let us consider the case that the density and temperature profiles of the hot electron are bell-shaped as,

$$n_h(r,z) = n_{ho}\, e^{-\kappa_n z - \eta_n^2 r^2}, \tag{3}$$

$$T_h(r,z) = T_{ho}\, e^{-\kappa_T z - \eta_T^2 r^2}, \tag{4}$$

where $\eta_{n,T}^2 \ll \kappa_{n,T}^2$. Equations (1), (3) and (4) give the fields. Since $\eta_{n,T}^2 \ll \kappa_{n,T}^2$ electric field is taken to be parallel to the z axis.

$$E_z = \frac{1}{e}(\kappa_T + \kappa_n) T_h \,,$$

$$\dot{B}_\theta = \frac{2}{e}(\kappa_T \eta_n^2 - \kappa_n \eta_T^2)\, \gamma\, T_h \,. \qquad (5)$$

Electromagnetic field is shown in Fig.1 schematically. Note that the direction of B field is determined by the anisotropy of the spatial hot electron distribution. From Eqs.(2) and(5) we obtain the energy of the ion accelerated along the z axis

$$\frac{1}{2} M v^2 = Z T_{h0} \left(1 + \frac{\kappa_n}{\kappa_T}\right)\left(1 - e^{-\kappa_T z}\right) + T_c \,, \qquad (6)$$

where T_c is the temperature of an unaccelerated ion. The kinetic energy of the ion reaches $T_c + Z(1+\kappa_n/\kappa_T) T_{h0} \equiv T_c + Z T_f$ which is about $Z(1+\kappa_n/\kappa_T)$ times greater than the energy of hot electron.

Then we show that ions are accelerated mainly along the magnetic null line in the case of $B_\theta > 0$.

Near the z axis $|E_z| \gg |v_r B_\theta|$, Eq.(2) becomes

$$\dot{v}_z = \frac{Z}{M}(\kappa_T + \kappa_n) T_{h0} e^{-\kappa_T z} \,, \qquad (7)$$

$$\dot{v}_r = -\frac{eZ}{M} v_z \int \dot{B}_\theta \, dt + r\dot{\theta}^2 \,. \qquad (8)$$

From Eq.(7),

$$v_z = \sqrt{\frac{2Z}{M}\left(\frac{T_c}{Z} + T_f - T_f e^{-\kappa_T z}\right)}. \qquad (7')$$

Equation of ion trajectry is obtained from Eqs.(7') and (8)

$$2\left(1+\frac{T_c}{ZT_f} - e^{-\kappa_T z}\right)\frac{d^2\gamma}{dz^2} + \kappa_T e^{-\kappa_T z}\frac{d\gamma}{dz}$$
$$= -2\beta\gamma\frac{T_{h0}}{T_f}F\left(1+\frac{T_c}{ZT_f}, \kappa_T z\right)\gamma + \frac{L^2}{2MT_f\gamma^3}, \qquad (9)$$

$$\beta \equiv \frac{\eta_n^2}{\eta_T^2} - \frac{\kappa_n}{\kappa_T}, \qquad \gamma \equiv \frac{\eta_T^2}{\kappa_T^2},$$

$$F(\alpha, x) = e^{-x}\sqrt{\alpha - e^{-x}}\int_0^x \frac{ds}{\sqrt{\alpha - e^{-s}}}.$$

where γ is a prameter which denotes an anisotropy of temperature profile and β denotes the difference between the anisotropies of density and temperature profiles and determines the sign of B_θ. Equation (9) is solved with following initial conditions and parameters: T_c=0.5keV, T_{h0}=20keV, Z=1~3, γ=0.1, β=-5~10, r(z=0)=0~r_0, $v_r = v_z \tan\varphi$ ($\varphi = 0 \sim \frac{\pi}{3}$), and L=0. The typical trajectries of ion are shown in Fig.2 for $B_\theta > 0$ (solid line) and for $B_\theta < 0$ (dashed line). Figure 2 shows the strong dependency of ion motion on the sign of B_θ. If $B_\theta > 0$ ions are converged and meandering [2] in the accelerating duct, if $B_\theta < 0$ ions diverge. High Z has a slight focusing effect.

Figure 3 shows the trajectries for ions accelerated a) from t=0 and b) t= $\tau_0 \equiv 1/v_c \kappa_T$ (characteristic acceleration time in the meandering duct).

Far outside the meandering duct, ion feels the small electric field and time dependent strong magnetic field. Taking $B_\theta = \dot{B}_\theta \tau_0$ at the original point t=0, $B = \dot{B}_\theta (t+\tau_0)$. Strictry speaking, τ_0 must be given for each ion. The gross property of the ion motion is investigated by giving an averaged value $\tau_0 = 1/v_c \kappa_T$ which is a characteristic acceleration time. In this situation, the field variation is small during its Larmor gyration. Though the trajectry of an ion is complicated, the averaged motion is given $\vec{E} \times \vec{B}$ and $\vec{B} \times \nabla \vec{B}$ drifts as

$$V_{Dr} = -\frac{E_z}{B_\theta} + \frac{M\langle v_\perp^2 \rangle}{2ZeB} \frac{(\vec{B} \times \nabla \vec{B})_r}{B^2}$$

$$= \frac{1}{(\tau_0 + t)\eta_T^2 \gamma} \cdot \frac{(1+\kappa_n/\kappa_T) T_h + T_\perp/2}{2(\kappa_n/\kappa_T - \eta_n^2/\eta_T^2) T_h} \Big/$$

$$\frac{d(\eta_T \gamma)}{dt} \sim O\left(-\frac{1}{\beta \tau_0 (\eta_T \gamma)}\right). \qquad (11)$$

Drift direction depends on the sign of B_θ. With positive B_θ field ion drifts inward to the duct, and negative B_θ makes an opposite drift motion. Once ion comes into the duct, the preceeding analysis is applied and ions become focused. [3]

Summary and Discussions

Summary of our investigation is ; 1 Ion is accelerated and is focused by the electromagnetic field generated by the hot electrons. 2 And its final energy is greater than the hot electron temperature by the factor $Z(1+\kappa_n/\mu_T)$. 3 These acceleration process strongly depends on the sign of the magnetic field, when $B_\theta > 0$, ion converges into the duct and is accelerated along the magnetic null line, on the other hand, when $B_\theta < 0$, ion may diverge and few ions are accelerated along the z axis. Our analysis is not selfconsistent: the electric field indeed is modified by the ion motion. But it does not change the essential physical picture of the process. More detailed numelical simulation and elaborate observations are desirable for a precise argument.

ACKNOWLEDGEMENTS

We wish to thank Professors T.Sato and A.Hasegawa for helpful discussions and all the members of Daisen Summer Seminor.

REFERENCES

[1] Valeo, E. J. and I. B. Bernstein, Preprint.

[2] Sonnerup, B. U . Ö, J. Geophys. Res. 76 8211 (1971).

[3] This focusing effect of B field may explain the experimental discrepancy about the existence of the fast ion.

FIGURE CAPTIONS

Fig. 1 The situation between the laser beam and plasma target and the direction of electromagnetic field are shown schematically. a) For $B_\theta > 0$, drift motions (both $\vec{E} \times \vec{B}$ and $\vec{B} \times \nabla \vec{B}$) of ions are inward to the axis. b) For $B_\theta < 0$, ions drift outward from the meandering duct and may diverge.

Fig.2 Ion trajectries for various initial conditions and parameters ; $Z=1$, $\gamma = 0.1$, $r(z=0)=0$, $r_0 / r_\theta = 0, 0.2$, $v_r = v_z \tan\varphi$ ($\varphi = 0, \frac{\pi}{6}, \frac{\pi}{3}$) and the original point of the time is $\tau_0 = 1/v_c \kappa_T$. Dashed lines indicate the case for $B_\theta < 0$ ($\beta = -3$) (Fig. 1 (b)) and solid lines show the case for $B_\theta > 0$ ($\beta = 5$) (Fig. 1 (a)).

Fig. 3 Ion trajectries with $z=1$, $\gamma = 0.1$, $r_0 = 0.2$, $\varphi = 0, \frac{\pi}{6}, \frac{\pi}{3}$, $\beta = -3$ (dashed line) and $\beta = 5$ (solid line) a) accelerated from t=0 and b) $t = \tau_0$.

Fig.1

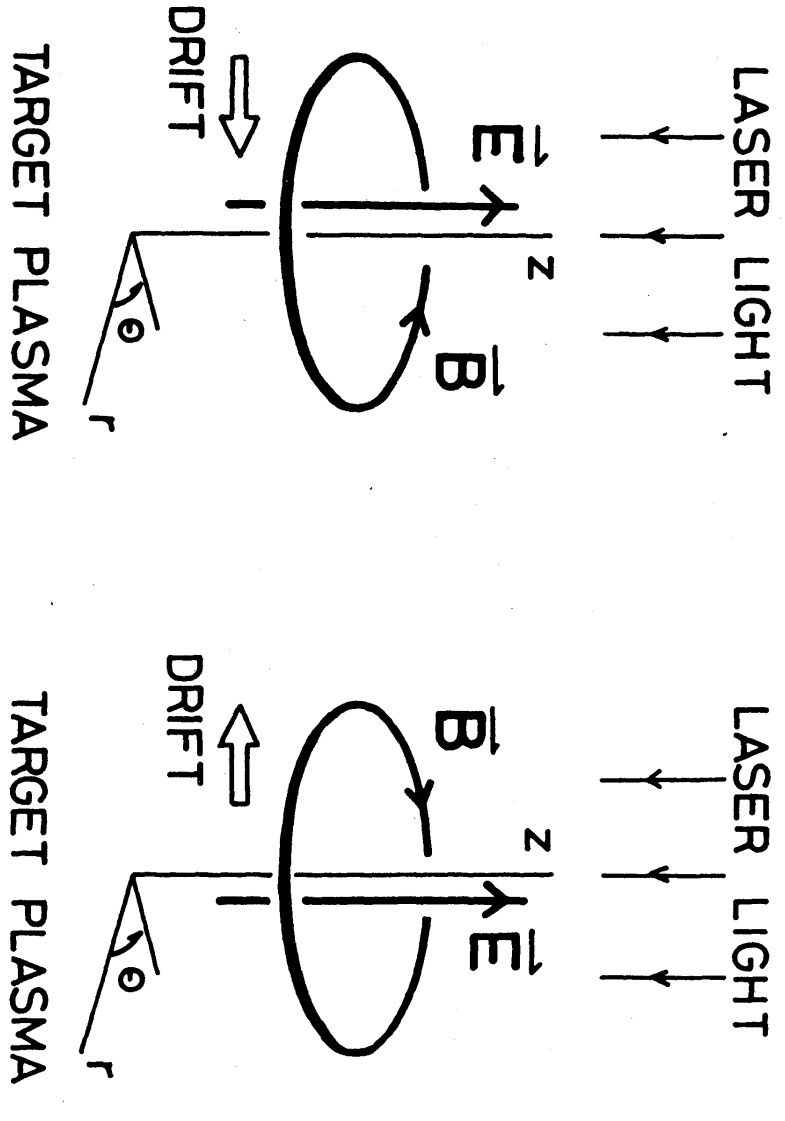
LASER LIGHT
E
B
z
DRIFT
TARGET PLASMA
θ
r
a)
LASER LIGHT
B
E
z
DRIFT
TARGET PLASMA
θ
r
b)

Fig.2

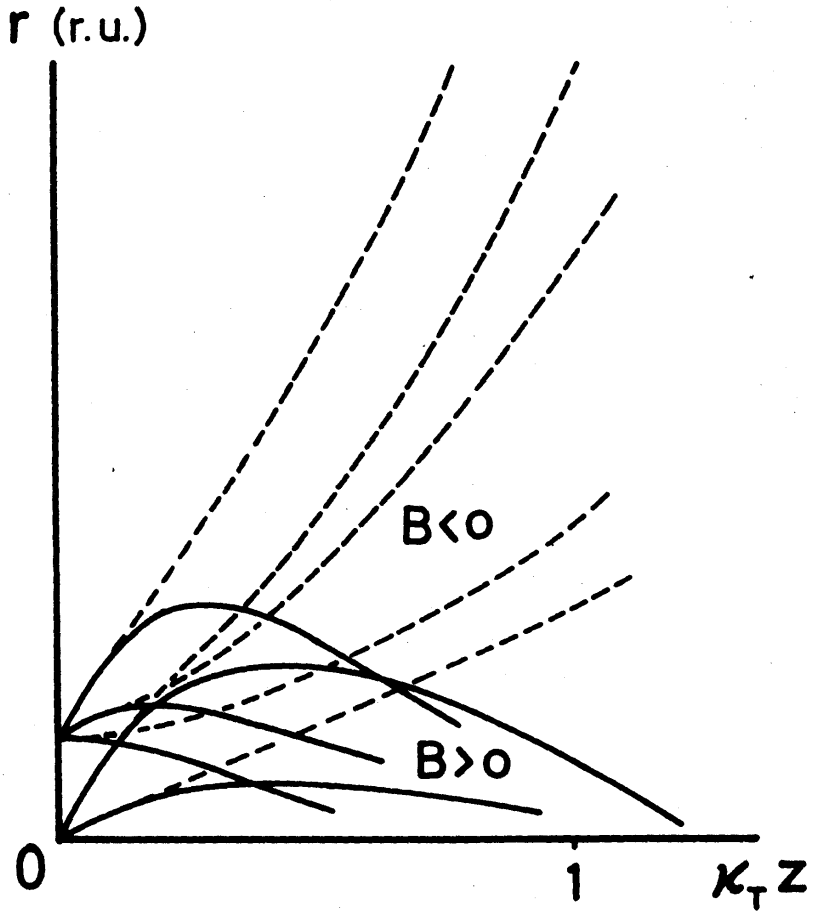

Fig.3

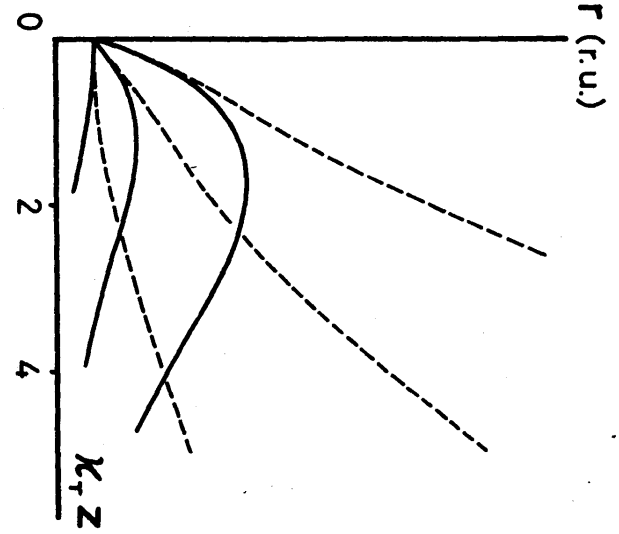

a)

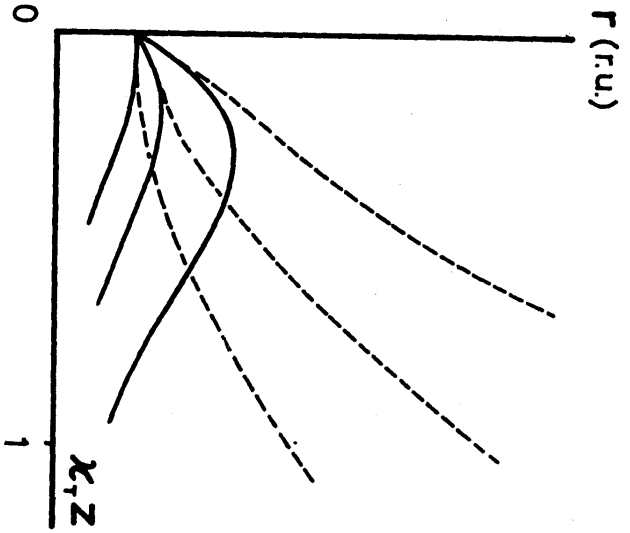

b)